

Measuring pure water absorption coefficient in the near-infrared spectrum (900—2500 nm)

DENG Ruru, HE Yingqing, QIN Yan, CHEN Qidong, CHEN Lei

School of Geography and Planning, Centre for Remote Sensing and Geographical Information Sciences, Sun Yat-sen University, Guangzhou 510275, China

Abstract: According to the extreme large and mutable characteristics of water absorption coefficient in the infrared spectrum, a device for measuring thin thickness of water layer is developed on the basis of the previously presented system for measuring water absorption coefficient in the optical region, in order to change the thickness of water layer from 0.04 mm to 350 mm. Then water absorption coefficient is measured with water layers of different thicknesses between 0.04 mm to 150 mm. After the effect of impurity was removed, measured data is integrated effectively and the absorption coefficient of pure water in spectrum from 900 nm to 2500 nm is obtained. Because the pure water absorption coefficient of each section in the spectrum is measured accurately under optimum detecting range of the instrument, the result is more reliable and agrees well with previous measurements. It can be used as basic data in quantitative remote sensing applications.

Key words: absorption coefficient, pure water, near-infrared spectrum, extinction coefficient

CLC number: TP701 **Document code:** A

Citation format: Deng R R, He Y Q, Qin Y, Chen Q D and Chen L. 2012. Measuring pure water absorption coefficient in the near-infrared spectrum (900—2500 nm). *Journal of Remote Sensing*, 16(1): 192–206

1 INTRODUCTION

Water is one of the most important and active substance on the earth and plays an important role in the nature of many physical, chemical and biological processes. In all the properties of water, absorption is the most important one. Therefore, the spectrum absorption of water is a remarkable parameter in chemical, biological, atmospheric sciences and many other fields of sciences which is also one of the crucial basic parameters in quantitative remote sensing. Previously, we introduced a new method for measuring the absorption coefficient of water in visible spectrum and illustrated the result of measurements from 400 nm to 900 nm. On the basis of that, this paper will extend the method to measure the absorption coefficient of water in the infrared spectrum ranges from 900 nm to 2500 nm.

It is very difficult to measure the absorption coefficient of water in the infrared spectrum because a large amount of energy in this region will be absorbed by water. Due to this reason, luminous intensity will become so weak that lights cannot be detected by sensors when going through water. Existing methods are not suitable. For obtaining successive absorption spectrum, in the meanwhile guaranteeing the precision of measurement, a sheet of water should be thin enough. According to the measurements in the infrared spectrum from Palmer and Williams (1974). The maximum thick-

ness of water layer is about 0.15 mm. However, due to the surface tension of water, it is almost impossible to make a sheet of thin water on glass like that.

Though many works focus on the measurements of absorption spectrum of water in the near infrared (Curcio & Petty, 1951; Hale & Querry, 1973; Palmer & Williams, 1974; Tyler & Querry, 1978; Wieliczka & Weng, 1989; Kou & Labrie, 1993; Gordon, 1993; Marley & Gaffney, 1994), there are obvious errors in the results of early results, as those integrated by Hale and Querry (1973). The widely accepted result was from Palmer and Williams (1974). Though the general procedures they employed also were, as earlier works, to measure the ratio of the reflectance of water to that of a reference mirror, and absorption coefficients were calculated from the reflectance. Water sample container they employed were a set of Infrasil quartz cells that provided path lengths of 1 to 50 mm, and a Beckmann variable-path-length cell that provided the path length in the range of 6 mm to 30 μm . So the precision of absorption coefficients they acquired in IR regions was very high.

Later studies improved the wedge-shaped cell for highly absorbent liquids by rising its versatility and avoiding the possible interference fringes from the wedge shaped volume between top and base of the window (Tyler, et al., 1978; Wieliczka, et al., 1989). Using the absorption cell with the optical path lengths in water ranging from 100 μm to 20 cm, Kou, et al. (1993) measured the

Received: 2011-07-27; **Accepted:** 2011-10-22

Foundation: National Natural Science Foundation of China (No.40671144); National High Technology Research and Development Program of China(863 program) (No.2006AA06Z416); Introduction of International Advanced Agricultural Science and Technology Projects of China (948 program) (No.200820)

First author biography: DENG Ruru (1963—), male, Ph.D., professor, his research interests are remote sensing for water quality and atmospheric environment. He has published more than 40 papers. E-mail: eesdr@mail.sysu.edu.cn

absorption spectrum in the region from 660 nm to 2500 nm, and the results were in good agreement with those obtained by Palmer and Williams. However, the measured absorption coefficient of water in 950 nm seems to be larger since scattering lights caused by some impurities in water have not been considered.

For some demanding applications, the existing measurements of water absorption coefficient in the infrared spectrum have some room to improve. As the data measured 37 years ago, Palmer and Williams's data is limited by the instrument, the lowest spectral resolution of the data is just tens of nanometers, so it is significantly insufficient for the applications of hyperspectral remote sensing. However, the result from Kou, et al. (1993) has a large value in the short-wave spectrum, and it will cause congenital error in some practical application. Therefore, it is necessary to measure the absorption coefficient of water accurately on the entire optical wave.

According to the nature of water absorption as well as the measurements of pervious studies, absorption coefficient of water has two characteristics: (1) the value of water absorption coefficient is very large; (2) the range of the values is wide. From visible to infrared spectra, absorption coefficient covers five orders of magnitude. In order to precisely measure the absorption coefficient of water, the following two aspects should be considered. (1) A very thin layer of water with the thickness less than 0.15 mm should be measured; (2) As to different wavelengths, the thickness of water should be measured according to the range of absorption coefficients to ensure the measured values falling in the effective range of devices.

Thus, based on the previous measurement system of water absorption coefficient, this study designed a special device for measuring thin layer of water. The device was feasible for measuring the thickness of water from 0.04 mm to 350 mm. Absorption coefficients at optimum detection ranges of the device for different wavelengths can be obtained by measuring the irradiance. After

data integration, we can get the absorption coefficients of pure water from visible to infrared wavelengths, i.e. from 400 nm to 2500 nm.

2 EXPERIMENT METHOD

2.1 Measurement device

The Measuring apparatus were introduced in Deng, et al. (2012). However, due to the surface tension of water, it is almost impossible to make the thickness of water layer on glass thinner than 0.5 mm. To measure the water absorption coefficient on the infrared wave band, as shown by Fig. 1, we control top surface of water layer with a sheet of even glass with high transparency. And two terminals of glass sheet are based with shims on the bottom of glass vat. Thickness of water layer is controlled by changing the type and number of the shims. There are four types of shims, two of them are rectangular stainless steel slice with thickness of 0.5 mm and 0.25 mm, respectively, the other two are rectangular film with thicknesses of 0.1 mm and 0.04 mm, respectively. Therefore, the thinnest water layer in the experiment is 0.04 mm, and it can easily be changed. With the means of experiment in optical spectrum, the thicknesses of water layer can vary from 0.04 mm to 150 mm in the experiment. Thus, it ensures that any absorption spectrum from 400 nm to 2500 nm is accurately measured by the optimum detected range of the instrument.

The water we used in test was ultrapure water, which is commercially supplied by National Marine Institute of China. The temperature during experiment was 26°C.

2.2 Measurement and calculation for near-infrared absorption coefficient of water measurement

The measurement method was similar to that in the visible spectrum, and we also measured the two water layers of different thicknesses to calculate the near-infrared absorption coefficient.

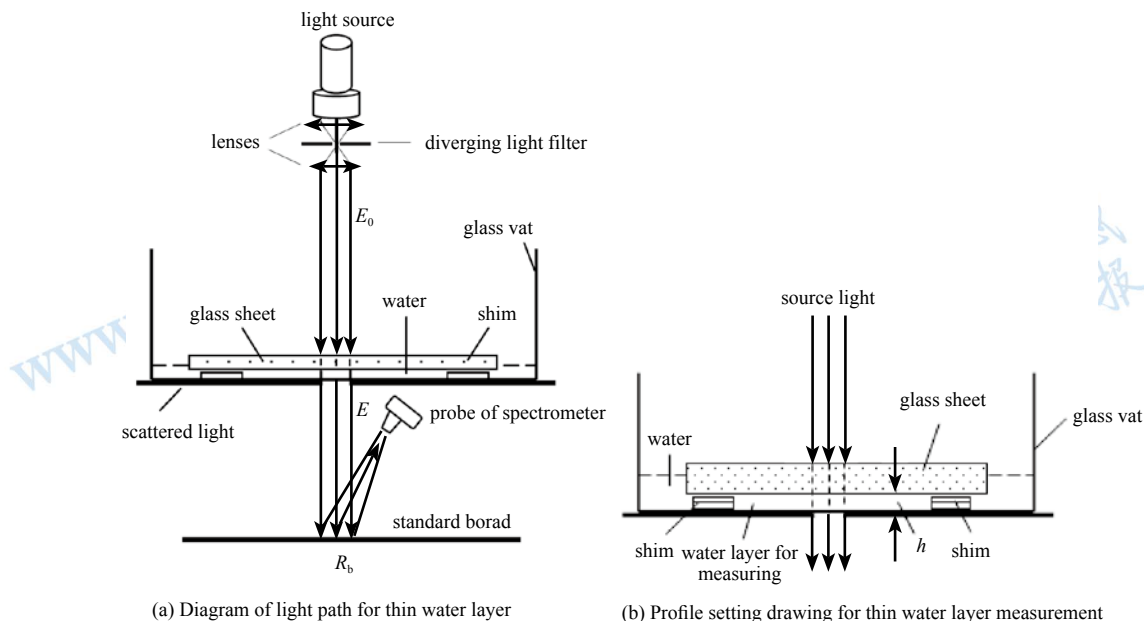


Fig. 1 The device for infrared spectrum

The data processing procedure also contained calibrating the data and separating absorption spectrum of pure water from the extinction coefficient of suspending substance. The detail of principle and methods of data processing procedure can be referenced to the paper (Deng, et al., 2012). After data calibration, the extinction coefficient of water can be expressed as:

$$k = \frac{1}{h_2 - h_1} \ln\left(\frac{L_1}{L_2}\right) \quad (1)$$

where h_1, h_2 are different thicknesses of two water layer samples, respectively, L_1, L_2 are the radiance corresponding detected by the spectrometer.

Then absorption coefficient of pure water can be calculated with the formula as:

$$\alpha_w(\lambda) = k(\lambda) - b_w(\lambda) - k_s(\lambda) \quad (2)$$

where $b_w(\lambda)$ is scatter ring coefficient of water molecule and $k_s(\lambda)$ is the extinction coefficient of suspended substance.

2.3 The union of absorption coefficients of pure water from 900 nm to 2500 nm

Measured absorption coefficient spectrum with different thicknesses of water layer has different characteristics of precision. The precisions of extinction coefficients measured with deep water layer are higher in low absorption region, but are lower in heavy absorption region, and precision of the measured values of water layer thickness are also higher, and vice verse. In fact, a definite thickness of water layer has a determinate optimal measured region of extinction coefficients value which is decided by the absorption of water, intensity of light source, and sensitivity of detecting instrument.

Because the values of absorption coefficient of water span five orders of magnitudes, it is necessary to get water absorption coefficient spectrum with high precision from the datum measured from different degrees of water thicknesses. So, combined the experiment of optical spectrum, the results measured with thickness between 0.04 mm to 150 mm are combined to make a union extinction coefficient spectrum of pure water over the spectrum of 350 nm to 2500 nm. The thicknesses of water layer measured in the

experiment are listed in Table 1.

For each thickness, we only chose the values which were in the best value range. All data ranges of adjacent measured water layer thicknesses have overlap parts of wavelength. Because the precisions of the value of measured water layer thickness are higher in larger thickness measurement, values of thickness of thin water layer are adjusted with a ratio according to the values of overlap region of data from larger thickness measurement. Finally, we acquired the absorption coefficient of pure water from 900 nm to 2500 nm with high precision.

Table 1 The thicknesses of water layer measured in the experiment/mm

thickness	thickness	thickness	thickness	thickness	thickness	thickness
0.04	0.30	0.80	3.00	20.00	70.00	120.00
0.08	0.40	0.90	3.50	30.00	80.00	130.00
0.12	0.50	1.00	4.00	40.00	90.00	140.00
0.16	0.60	1.50	5.00	50.00	100.00	150.00
0.20	0.70	2.00	10.00	60.00	110.00	

3 ABSORPTION DATA AND ERROR DISCUSSION

3.1 Data processing

More than 20 sets of measured data of same thickness of water layer were averaged to get the result of absorption spectrum, and statistics standard deviation and percent error were also calculated. The standard deviation for the new absorption value a_i is

$$\sigma_{a_i} = \frac{(1/\sigma_{i-1}^2 + 4/\sigma_i^2 + 1/\sigma_{i+1}^2)^2}{1/\sigma_{i-1}^2 + 2/\sigma_i^2 + 1/\sigma_{i+1}^2} \quad (3)$$

The final results were shown in Appendix Table. At each wavelength, values were given for the absorption coefficient as well as its statistical standard deviation. The absorption coefficient is also shown in Fig. 2. As indicated in the figure, the values of absorption coefficient of water at 400 nm to 2500 nm differ by a factor of 10^5 ; the bars of uncertainty for various spectral regions are also indicated in the Fig. 2.

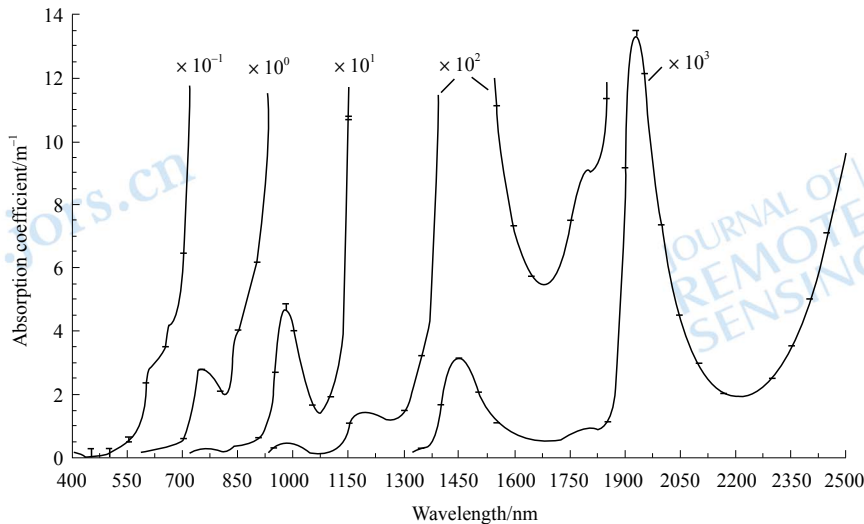


Fig. 2 Unioned absorption coefficients of pure water between 400 nm and 2500 nm

3.2 Comparison with previous studies

The final results of absorption coefficient on 400 nm to 2500 nm are shown in Fig. 3 to compare with those from Smith and Baker (1981), Pope and Fry (1997), Sogandares and Fry (1997), Hale and Querry (1973), Kou, et al. (1993) and Palmer and Williams (1974).

Absorption spectrum of pure water from Pope and Fry, and Palmer and Williams are widely accepted absorption spectrum of pure water on spectrum of optical and infrared regions respectively. Fig. 3 shows that the results of this paper are generally highly correlated with the datum from Pope and Fry, and Smith and Baker on 450 nm to 700 nm region, and with the datum from Palmer and Williams, and Kou and Labrie and Chylek on 750 nm to 2500 nm region. In the last paper we have made the comparison for spectrum from 400 nm to 900 nm, so we do not repeat here. In the peak

area of infrared spectrum, where the results are different from each other, our results are usually between Palmer and Williams's and Kou, Labrie and Chylek's (1993), and closer to the latter. The absorption coefficients of water around 1930 nm are the most typical. As shown in Fig. 3, our results are significantly greater than Palmer and Williams's around 1930 nm, but slightly smaller than Kou, Labrie and Chylek's. The values on 1925 nm are 13285, 12400 and 13470, respectively. When measuring absorption coefficient on a certain region, it is inclined to increase the thickness of measured water layer to insure the good precision of results in the general region. While it is likely to make the light energy penetrating through water layer on the peak region of absorption too little and out of optimal range of detecting. Thus, it implies that the measurements of absorption coefficient are unstable. However, in our work, all regions of absorption coefficient are measured in optimal range of detecting, ensuring more stable measurements.

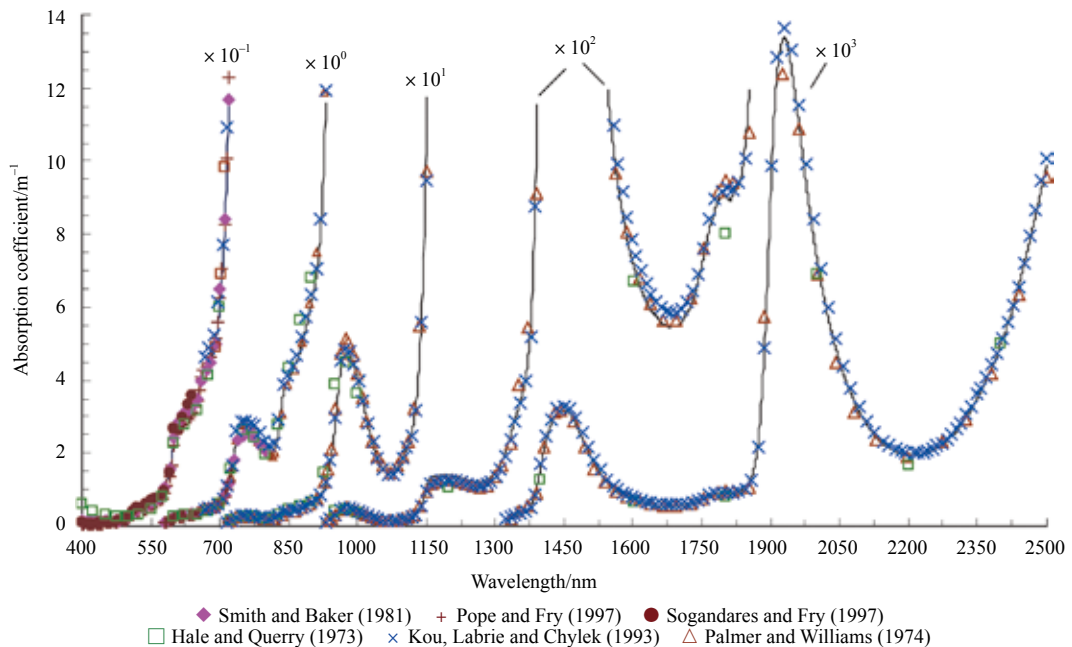


Fig. 3 Present results (smooth curve) for the absorption of pure water between 400 nm and 2500 nm plotted with other researchers

4 SUMMARY

A new method of the measurement for absorption coefficients in the infrared spectrum of pure water is put forward. Besides simple and direct, this method are easy to control the thickness of measured water layers, the thicknesses can be measured span 0.04 mm to 350 mm, so all region of optical and large part of IR can be measured available.

Using the method of ratio to calculate the absorption coefficients of water, the main factors of light source and instrument were removed effectively.

Based on the measurements to water layer with thickness from 0.04 mm to 350 mm, absorption coefficients spectrum of pure water in region of 400 nm to 2500 nm are obtained. Since the data in each region of wavelength is acquired in the optimal detecting range of water depths, the precision is reliable and the results have a good correspondence with widely accepted results.

REFERENCES

- Curcio JA and Petty C C. 1951. The near infrared absorption spectrum of liquid water. *Journal of the Optical Society of America*, 41(5): 302–304
- Deng R R, He Y Q, Qin Y, Chen Q D and Chen L. 2012. Pure water absorption coefficient measurement eliminating the impact of suspended substance in spectrum from 400 nm to 900 nm. *Journal of Remote Sensing*, 16(1):174–191
- Gordon H R. 1993. Sensitivity of radiative transfer to small-angle scattering in the ocean: quantitative assessment. *Applied Optics*, 32(36): 7505–7511
- Hale G M and Querry M R. 1973. Optical constants of water in the 200nm to 200μm wavelength region. *Applied Optics*, 12(3): 555–563
- Kou L H, Labrie D and Chylek P. 1993. Refractive indices of water and ice in the 0.65- to 2.5-μm spectral range. *Applied Optics*, 32(19): 3531–3540

- Marley N A, Gaffney J S and Cunningham M M. 1994. Lambert absorption coefficients of water in the frequency range of 3000-934 cm⁻¹. *Applied Optics*, 33(34): 8041-8054
- Palmer K F and Williams D. 1974. Optical properties of water in the near infrared. *Journal of the Optical Society America*, 64(8): 1107-1110
- Pope R M and Fry E S. 1997. Absorption spectrum (380-700 nm) of pure water. II. Integrating cavity measurements. *Applied Optics*, 36(33): 8710-8723
- Smith R C and Baker K S. 1981. Optical properties of the clearest natural waters. *Applied Optics*, 20(2): 177-184
- Sogandares F M and Fry E S. 1997. Absorption spectrum (340-640 nm) of pure water. 1. Photothermal measurements. *Applied Optics*, 36(33): 8699-8709
- Tyler I L, Taylor G and Querry M R. 1978. Thin-wedge-shaped cell for highly absorbent liquids. *Applied Optics*, 17(6): 960-963
- Wieliczka D M, Weng S S and Querry M R. 1989. Wedge shaped cell for highly absorbent liquids: infrared optical constants of water. *Applied Optics*, 28(9): 1714-1719

Appendix Table

Absorption Coefficients α_w and standard Deviations σ , for pure water as a function of wavelength λ

λ/nm	α_w/m^{-1}	σ/m^{-1}	λ/nm	α_w/m^{-1}	σ/m^{-1}	λ/nm	α_w/m^{-1}	σ/m^{-1}
900	6.1884	0.0256	1090	16.6783	0.5654	1280	125.4438	3.8587
905	6.5073	0.0235	1095	17.8467	0.5888	1285	128.5339	3.9124
910	6.9042	0.0184	1100	19.2845	0.5352	1290	132.9452	4.0090
915	7.4607	0.0128	1105	20.8313	0.5112	1295	138.8124	4.1269
920	8.3139	0.0167	1110	22.5262	0.5184	1300	145.8619	4.2425
925	9.6392	0.0322	1115	24.4669	0.5060	1305	154.6123	4.4000
930	11.5774	0.0556	1120	27.0585	0.5441	1310	165.8897	4.5936
935	14.1677	0.0876	1125	31.0228	0.6470	1315	179.8041	4.8251
940	17.3963	0.1492	1130	37.3991	0.8985	1320	195.9858	5.0714
945	21.4374	0.2885	1135	47.1984	1.3243	1325	214.5301	5.3591
950	27.0426	0.2617	1140	60.7775	2.0327	1330	235.1264	5.6463
955	33.9925	0.5221	1145	79.6172	1.6023	1335	257.4468	5.9333
960	40.4604	0.8134	1150	107.4252	3.6212	1340	280.2109	6.2337
965	44.6345	1.0380	1155	125.5627	3.8223	1345	301.8872	6.4778
970	46.5729	1.2266	1160	131.6432	3.9251	1350	322.9455	6.7370
975	47.2258	1.4434	1165	134.8601	3.9844	1355	343.8465	6.9696
980	47.1185	1.1067	1170	136.6320	4.0448	1360	367.4948	7.2164
985	46.1659	1.2028	1175	137.6525	4.0541	1365	399.2005	7.5428
990	44.5386	1.1441	1180	138.5555	4.0835	1370	443.8689	7.9816
995	42.4961	0.9612	1185	139.4848	4.0822	1375	508.1205	8.5702
1000	40.0382	0.5827	1190	140.4580	4.1114	1380	614.3273	10.8652
1005	37.4344	0.5687	1195	140.7465	4.1106	1385	791.0386	12.4317
1010	34.7226	0.5942	1200	140.2052	4.1212	1390	1037.7462	14.2865
1015	31.7971	0.4985	1205	139.2073	4.1050	1395	1338.3514	16.2805
1020	28.9374	0.5549	1210	137.7093	4.0651	1400	1671.4614	18.2428
1025	26.2427	0.5029	1215	136.1539	4.0459	1405	2004.7756	20.0347
1030	23.8181	0.5161	1220	134.5039	4.0094	1410	2299.4013	21.4677
1035	21.6558	0.5049	1225	132.5723	3.9777	1415	2546.4080	22.5945
1040	19.6868	0.4859	1230	130.8398	3.9402	1420	2742.4414	23.4508
1045	18.0350	0.4833	1235	129.0345	3.9052	1425	2888.7492	24.0617
1050	16.7533	0.4719	1240	127.1222	3.8697	1430	2998.7826	24.5045
1055	15.7747	0.4739	1245	125.4440	3.8483	1435	3077.4039	24.8265
1060	15.0632	0.4630	1250	123.9184	3.8271	1440	3125.9429	25.0176
1065	14.6171	0.4657	1255	122.6804	3.7974	1445	3149.9303	25.1116
1070	14.4471	0.4698	1260	121.8107	3.7821	1450	3159.1215	25.1574
1075	14.5493	0.4951	1265	121.6186	3.7675	1455	3145.7882	25.0872
1080	14.9843	0.5006	1270	121.9652	3.7863	1460	3104.6653	24.9376
1085	15.7179	0.5281	1275	123.1212	3.8046	1465	3032.2772	24.6450

to be continued

continue								
λ/nm	α_w/m^{-1}	σ/m^{-1}	λ/nm	α_w/m^{-1}	σ/m^{-1}	λ/nm	α_w/m^{-1}	σ/m^{-1}
1470	2921.7997	24.1834	1715	580.7795	10.6598	1960	11174.4059	47.3403
1475	2789.9066	23.6105	1720	588.9609	10.7467	1965	10658.6376	46.1908
1480	2649.0557	23.0134	1725	600.8988	10.8644	1970	10110.3070	44.9694
1485	2503.1788	22.3575	1730	619.2023	11.0118	1975	9587.2335	43.8239
1490	2359.6925	21.7063	1735	640.1112	11.1797	1980	9093.3448	42.6545
1495	2216.7008	21.0201	1740	666.0047	11.4651	1985	8638.8885	41.5737
1500	2083.1254	20.3850	1745	689.4827	11.6367	1990	8201.0527	40.4800
1505	1955.5434	19.7313	1750	717.1088	11.8595	1995	7770.3487	39.4536
1510	1828.2567	19.0580	1755	752.7150	12.1704	2000	7364.6545	38.3348
1515	1707.3415	18.4441	1760	780.9415	12.3969	2005	6994.7081	37.3859
1520	1598.2384	17.8236	1765	809.3959	12.6638	2010	6647.0382	36.4063
1525	1501.0728	17.2870	1770	831.2326	12.8079	2015	6327.5106	35.5869
1530	1411.4466	16.7300	1775	849.2241	12.9889	2020	6007.5693	34.6112
1535	1330.0455	16.2448	1780	873.9375	13.1127	2025	5700.9784	33.7455
1540	1253.0276	15.7670	1785	894.0727	13.3086	2030	5421.2357	32.8879
1545	1178.4295	15.2867	1790	898.4171	13.3062	2035	5183.3520	32.1964
1550	1113.1924	14.8645	1795	902.1133	13.3612	2040	4953.4561	31.4398
1555	1056.4427	14.4633	1800	905.1582	13.3709	2045	4726.1692	30.7026
1560	1001.8636	14.0780	1805	899.7925	13.3183	2050	4512.3844	30.0040
1565	947.6307	13.6833	1810	891.7933	13.2702	2055	4302.5010	29.3131
1570	903.3081	13.3519	1815	901.2435	13.2675	2060	4114.0033	28.6546
1575	869.4973	13.1107	1820	916.9734	13.4471	2065	3949.8433	28.0594
1580	830.8426	12.7912	1825	922.1306	13.4119	2070	3791.7650	27.4838
1585	795.2601	12.5247	1830	934.6580	13.4713	2075	3636.0017	26.9347
1590	765.3087	12.2887	1835	953.4940	13.6030	2080	3483.4019	26.3476
1595	739.2764	12.0821	1840	994.0810	13.9207	2085	3335.0891	25.7767
1600	718.1947	11.8895	1845	1056.5967	14.3174	2090	3199.6813	25.2807
1605	698.1034	11.7092	1850	1132.9730	14.8648	2095	3080.8073	24.7402
1610	676.3345	11.5382	1855	1243.1728	15.5692	2100	2979.6127	24.3419
1615	656.8966	11.3502	1860	1415.7472	16.6691	2105	2881.9971	23.9525
1620	640.3602	11.2004	1865	1664.4644	18.0279	2110	2775.0513	23.4428
1625	624.4244	11.0867	1870	2067.3102	20.1143	2115	2692.1798	23.1439
1630	612.9789	10.9950	1875	2678.7960	22.9734	2120	2611.2278	22.7564
1635	600.3195	10.8386	1880	3500.1258	26.3717	2125	2526.6678	22.4146
1640	587.2072	10.7111	1885	4593.0215	30.1578	2130	2439.7979	21.9963
1645	581.5459	10.6964	1890	5992.0760	34.5577	2135	2367.2879	21.6851
1650	576.4747	10.6264	1895	7566.6078	38.9982	2140	2312.0539	21.4561
1655	566.8229	10.5321	1900	9196.2681	43.0143	2145	2256.0577	21.1354
1660	557.8632	10.4569	1905	10673.2160	46.3941	2150	2215.8617	20.9544
1665	552.4071	10.4134	1910	11785.0118	48.7745	2155	2177.0876	20.8096
1670	550.8155	10.4267	1915	12538.9739	50.2398	2160	2130.1240	20.5180
1675	546.4029	10.2933	1920	13019.8819	51.1522	2165	2099.8806	20.4763
1680	545.7660	10.3457	1925	13284.4851	51.7008	2170	2053.4546	20.1573
1685	548.7931	10.3422	1930	13377.2446	51.8120	2175	2024.7078	20.0260
1690	550.1508	10.3955	1935	13284.6730	51.6623	2180	2015.4595	20.0432
1695	548.1242	10.3343	1940	12985.2155	51.0066	2185	1995.7610	19.8553
1700	551.5667	10.4226	1945	12569.8817	50.2162	2190	1967.3868	19.7351
1705	557.4718	10.4550	1950	12121.3278	49.2982	2195	1944.7839	19.6313
1710	567.9853	10.5116	1955	11660.7820	48.3564	2200	1947.3039	19.6494

to be continued

continue

λ/nm	α_w/m^{-1}	σ/m^{-1}	λ/nm	α_w/m^{-1}	σ/m^{-1}	λ/nm	α_w/m^{-1}	σ/m^{-1}
2205	1953.0090	19.6160	2305	2600.9227	22.7054	2405	5170.8675	32.1701
2210	1976.9291	19.8194	2310	2694.8454	23.1953	2410	5266.7612	32.2945
2215	1967.1752	19.6807	2315	2789.5631	23.5403	2415	5519.1696	33.2164
2220	1962.5190	19.7697	2320	2887.5870	23.9247	2420	5695.1827	33.6903
2225	1962.7188	19.6689	2325	3009.1713	24.3983	2425	5886.0474	34.2915
2230	1958.9635	19.7425	2330	3077.0556	24.8207	2430	6106.4604	34.9973
2235	1992.9890	19.8530	2335	3151.8896	25.0671	2435	6342.7058	35.1967
2240	2032.2671	20.0908	2340	3289.8315	25.6099	2440	6583.8864	35.8459
2245	2038.9316	20.1235	2345	3408.2837	26.0753	2445	6830.0022	36.8070
2250	2070.8117	20.2535	2350	3522.2109	26.3853	2450	7081.0532	37.3600
2255	2110.6788	20.4194	2355	3642.7963	27.1051	2455	7337.0394	38.0974
2260	2137.1224	20.5265	2360	3770.5952	27.3852	2460	7597.9608	38.9928
2265	2172.9845	20.7662	2365	3890.6802	27.8528	2465	7863.8175	39.2615
2270	2207.9950	21.0225	2370	4015.3320	28.3421	2470	8134.6093	40.3983
2275	2248.7080	21.0766	2375	4165.6284	28.7980	2475	8410.3364	42.0815
2280	2299.6275	21.3013	2380	4282.6965	29.2605	2480	8690.9987	40.1862
2285	2373.7696	21.7304	2385	4426.6887	29.6833	2485	8976.5962	43.7344
2290	2442.6123	22.0061	2390	4603.4652	30.2149	2490	9267.1289	39.5020
2295	2491.4185	22.2091	2395	4794.8223	30.9753	2495	9562.5969	42.0205
2300	2548.7591	22.6158	2400	5032.0681	31.6918	2500	9863.0000	43.8201

近红外波段(900—2500 nm)水吸收系数测量

邓孺孺, 何颖清, 秦雁, 陈启东, 陈蕾

中山大学 地理科学与规划学院, 广东 广州 510275

摘要: 根据水在红外波段强吸收且吸收能力变化大的特点, 在所提出可见光波段水吸收系数测量系统基础上增设了薄层水测量装置, 使得测量水层厚度可在0.04—350 mm之间变化。在此基础上对厚度为0.04—150 mm的多个厚度水层进行了吸收系数测量, 并对消除杂质影响后的测量数据进行了有效整合, 得到900—2500 nm波段纯水吸收系数。由于确保了各波段数据均在仪器最佳探测区间取得, 所得结果精度较高, 且与被普遍接受的前期研究结果相一致, 可作为相关定量遥感的基础数据。

关键词: 吸收系数, 纯水, 近红外波段, 消光系数

中图分类号: TP701 **文献标志码:** A

引用格式: 邓孺孺, 何颖清, 秦雁, 陈启东, 陈蕾. 2012. 近红外波段(900—2500 nm)水吸收系数测量. 遥感学报, 16(1): 192—206
Deng R R, He Y Q, Qin Y, Chen Q D and Chen L. 2012. Measuring pure water absorption coefficient in the near-infrared spectrum (900—2500 nm). Journal of Remote Sensing, 16(1): 192—206

1 引言

水是地球环境中最重要, 也是最活跃的物质之一, 在自然界许多物理化学和生物过程中扮演着重要角色。而水的吸收是其最重要的性质。故水吸收光谱是化学、生物和大气等许多科学领域中的重要参数, 也是定量遥感最重要的基础参数之一。在前一篇文章中, 我们介绍了一种新的光学波段水吸收系数测量方法, 给出了400—900 nm波段水吸收系数的测量结果。本文将在此基础上进行进一步地扩展, 将水吸收系数的测量扩展至900—2500 nm的红外波段。

红外波段水吸收系数测量甚为困难, 其原因是该波段水吸收系数值非常大。由于水的超强吸收, 红外光穿透一定厚度的水体后光强往往很弱, 以致低于探测器所能探测到的最小值。因此, 一般的测量方法均不适用。要想获取连续的红外吸收系数光谱, 同时确保结果的精度, 必须要能对足够薄的水层进行测量, 根据Palmer和Williams(1974)等的水红外波段光学厚度测量值, 最低限度的水层厚约为0.15 mm。然而,

由于水的表面张力, 在一般的玻璃表面上, 获得低于1.5 mm的薄层水都是非常困难的。

有许多学者(Curcio和Petty, 1951; Hale和Query, 1973; Palmer和Williams, 1974; Tyler等, 1978; Wieliczka等, 1989; Kou等, 1993; Gordon, 1993; Marley等, 1994)对于红外波段水体吸收系数的测量做了大量工作, Hale和Query(1973)对这些结果进行了整合, 认为前人的结果存在比较大的误差。目前被普遍接受的结果来自Palmer和Williams(1974)。虽然采用的方法和早期的研究工作差异不大, 即通过测量水体和一个参考镜面反射率的比值, 进而算出水体的吸收系数, 但他们实验中所采用的水体样品容器有两种: 一种为一系列不同大小的红外石英楔子, 其水层的光路长度为1—50 mm; 另一种为贝克曼距离可调的楔子, 其水层的光路长度为6 mm—30 μm 。所以他们在红外波段测得的吸收系数的精度较高。

Tyler等人(1978)以及Wieliczka等人(1989)改进了承载水体的楔形单元, 提高其可调节性能, 避免了楔形体窗口由于顶底距离差异而产生的干涉条纹, 可用

收稿日期: 2011-07-27; 修订日期: 2011-10-22

基金项目: 国家自然科学基金(编号: 40671144); 国家高技术研究发展计划(863计划)(编号: 2006AA06Z416); 引进国际先进农业科学技术计划(948项目)(编号: 200820)

第一作者简介: 邓孺孺(1963—), 男, 博士, 教授, 博士生导师。主要从事水质遥感与大气环境遥感, 已发表论文40余篇。E-mail: eesdr@mail.sysu.edu.cn。

于强吸收液体的吸收系数测量。Kou等人(1993)采用水层厚度100 μm —200 mm的楔子,测量了660—2500 nm的纯水吸收光谱,测量值和Palmer、Williams的结果较为吻合。然而,由于没有考虑水中杂质散射光的影响,在波长小于950 nm的波段,其水吸收系数测量值明显偏高。

对于某些要求较高的应用来说,现有的红外波段水吸收系数测量结果均有一定的提升空间。作为测量于37年前的数据,Palmer和Williams的数据受当时仪器条件的限制,光谱分辨率最低部分仅为数十纳米,对于高光谱遥感等方面的应用而言明显偏低;而Kou, Labrie和Chylek等的测量结果在较短波段部分值偏大的趋势亦会在实际应用中产生一定的先天误差。故对整个光学波段水吸收系数进行更高精度的测量仍是十分必要的。

根据红外波段水吸收性质和前人测量的结果,可知该波段水吸收系数具有两个特点,一是吸收系数值极大;二是值的变化极大,从可见光到红外波段,水吸收系数的值跨越了5个数量级。故水吸收系数的精确测量必须要做到以下两个方面:一是要能测量极薄的水层,可测最小厚度小于0.15 mm;二是对不同的波段,根据吸收系数的数值区间需要测量不同厚度的水层,以保证数值在仪器的有效测量范围内。

由此,本文在之前可见光波段实验装置的基础上,设计了一套测量薄层水的特殊装置,可测量的最薄水层达到了0.04 mm。从而可对厚度为0.04—150 mm的水层进行测量。通过对不同厚度水层的测量,获

取由仪器最优探测区间测量得到的不同波段水吸收系数,再经过数据整合,获得从可见光到红外波段400—2500 nm波段的纯水吸收系数。

2 实验方法

2.1 测量装置

测量的基本装置以及仪器参见邓孺孺等人(2012)。由于水表面张力很大,要想获取厚度小于0.5 mm的水层,直接在玻璃容器中加入待测水体是无法得到的。因此,我们对测量装置进行了改进。如图1(a)、(b)所示,先在玻璃容器中加入少量的水,将一块高透过率的玻璃平板放在水表面,注意水层厚度不要超过玻璃板厚度;在玻璃板两端垫上类型、数量相等的若干长条形垫片,垫片置于在玻璃容器的底部。通过改变垫片的类型和数量即可改变待测水层的厚度。实验中一共使用了4种类型的垫片,其中两种是厚度分别为0.5 mm和0.25 mm的不锈钢片,另外两种是厚度分别为0.1 mm和0.04 mm的聚脂薄膜片。所以实验中能够测量的最薄水层为0.04 mm,而且可以很方便地改变测量水层的厚度。结合原可见光波段的测量方法,使得可测量水层的厚度变化区间达到0.04—150 mm。从而可以保证400—2500 nm的波长范围内任何波段的吸收光谱都可以仪器的最佳探测区间得到准确测量。

实验中所用的纯水是由中科院南海所提供的超纯水。实验在恒温26 $^{\circ}\text{C}$ 下进行。

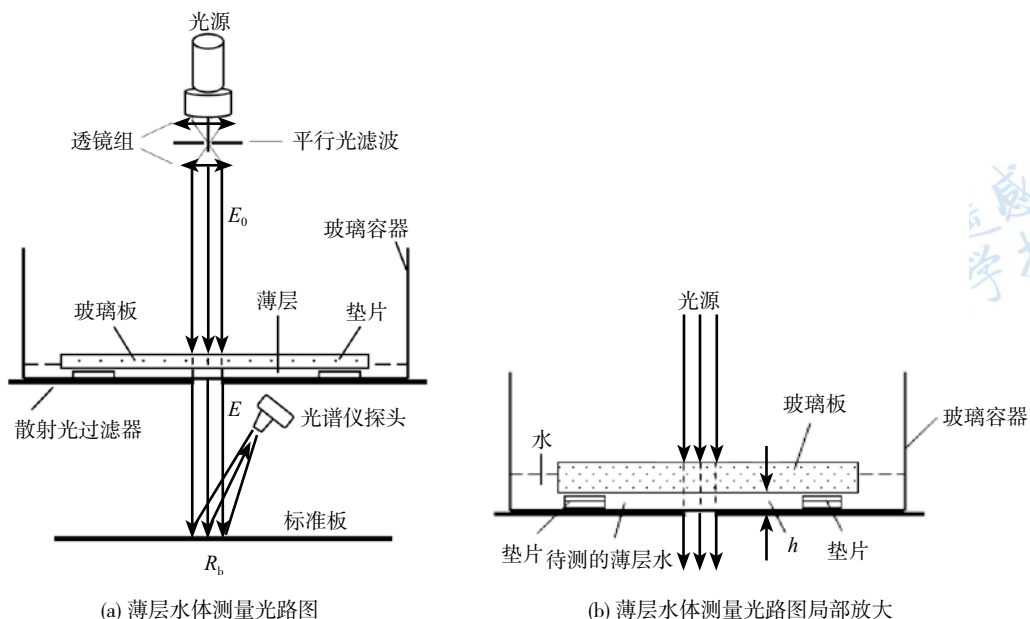


图1 红外波段测量装置

2.2 近红外波段水吸收系数的测量与计算

与可见光波段水吸收系数的测量方法相似, 亦采用对不同厚度水层的测量来计算近红外波段吸收系数。其间也需要进行数据纠正和除去水中悬浮杂质的影响。具体原理和数据处理方法请参阅(邓孺孺 等, 2012)文献。经过数据纠正后水体消光系数可表示为:

$$k = \frac{1}{h_2 - h_1} \ln\left(\frac{L_1}{L_2}\right) \quad (1)$$

式中, h_1 、 h_2 分别为两次测水层的厚度, L_1 、 L_2 分别为两次光谱仪探测到的相应辐亮度。纯水吸收系数计算公式为:

$$\alpha_w(\lambda) = k(\lambda) - b_w(\lambda) - k_s(\lambda) \quad (2)$$

式中, b_w 和 k_s 分别为水分子散射系数和水中悬浮粒子的消光系数。二者的计算方法在邓孺孺等人(2012)一文中已有详细介绍, 在此不再赘述。

2.3 900—2500 nm水吸收系数的整合

对不同厚度的水层测量得到的水吸收系数, 其精度也将不同。使用较厚水层测量所得吸收系数值, 在吸收系数小的波段精度较高, 在吸收系数大的波段精度较低, 且对水层厚度测量值的精度也较高; 反之, 使用较薄水层测量所得吸收系数, 在吸收系数大的波段精度较高, 在吸收系数小的波段精度较低, 同时水层厚度的测量值也容易出现误差。实际上, 每一确定厚度的水层都有一个测量消光系数的最佳取值区间, 这个区间由水的吸收系数、光源强度和仪器的灵敏区所决定。

由于水吸收系数的数值在可见光至近红外波段跨越5个数量级, 要想得到高精度的水体吸收系数, 必须对多个厚度的水层进行测量。因此, 结合可见光的

实验, 本文对厚度从0.04—150 mm的纯水层进行光谱测量, 然后通过上述方法计算得到350—2500 nm范围内相应波段的纯水吸收系数。所测量水层的厚度如表1。

对每一厚度水层的测量结果, 只取其最佳取值区间的结果进行整合。相邻厚度的水层测得的吸收系数, 在最佳波长区域上会有重叠的部分。在可见光波段, 所测水层厚度数据在水层厚度较大时精度较高, 所以根据重叠区域较厚水层所测数据, 对较薄水层所测的数据进行一定比例的调整。最后得到900—2500 nm波段具有较高精度的纯水吸收系数。

表1 实验测量水层厚度 /mm

水层厚度	水层厚度	水层厚度	水层厚度	水层厚度	水层厚度	水层厚度
0.04	0.30	0.80	3.00	20.00	70.00	120.00
0.08	0.40	0.90	3.50	30.00	80.00	130.00
0.12	0.50	1.00	4.00	40.00	90.00	140.00
0.16	0.60	1.50	5.00	50.00	100.00	150.00
0.20	0.70	2.00	10.00	60.00	110.00	

3 水吸收系数测量结果及误差分析

3.1 数据处理

与400—900 nm水吸收系数测量实验中的数据处理方式相同, 对某一确定厚度的水层, 同样需要利用超过20组测量数据取平均值, 才得到吸收光谱的结果, 并计算出标准差。标准差可由下式计算:

$$\sigma_{a_i} = \frac{(1/\sigma_{i-1}^2 + 4/\sigma_i^2 + 1/\sigma_{i+1}^2)^2}{1/\sigma_{i-1}^2 + 2/\sigma_i^2 + 1/\sigma_{i+1}^2} \quad (3)$$

附录表格列出了900—2500 nm波段的最终的水吸收系数测量结果。每一个波长都给出了相应的吸收系数以及标准差。图2中为400—2500 nm纯水吸收系

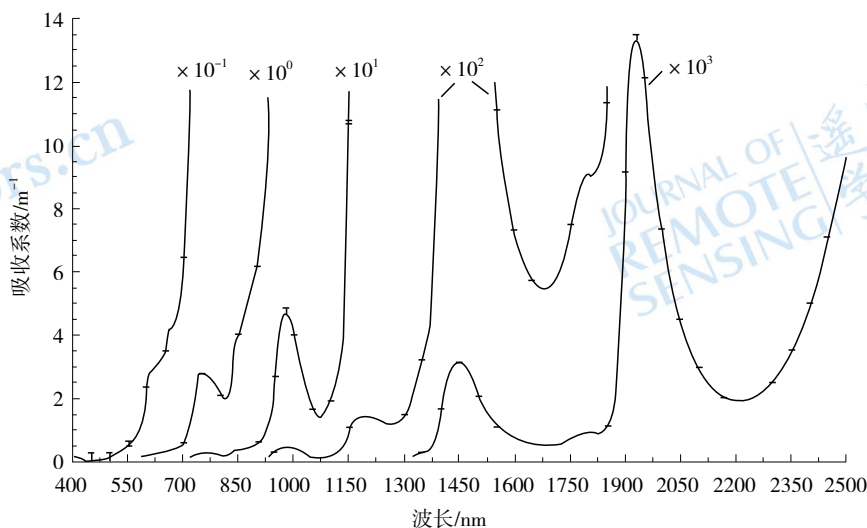


图2 400—2500 nm纯水吸收光谱曲线

数光谱曲线(400—900 nm的数值请参阅(邓孺孺等, 2012))。正如图2所示, 波长从400—2500 nm处, 水的吸收系数在数值上最大相差 10^5 。图2中也绘出了不同光谱区误差线。

3.2 与较早研究成果的对比

图3为本文所得的纯水400—2500 nm吸收系数测量结果与Smith和Baker (1981), Pope和Fry (1997), Sogandares和Fry (1997), Hale和Query (1973), Kou等(1993)以及Palmer和Williams (1974)的结果的对比。

Pope和Fry以及Palmer和Williams所得的纯水吸收光谱分别在可见光和红外波段范围内得到广泛认可。图3显示了本文的结果与Pope和Fry、Smith和Baker在450—700 nm波谱范围的结果以及Palmer和Williams, Kou、Labrie和Chylek在750—2500 nm波谱范

围的结果总体上高度一致, 但在部分峰值区存在一定的差异。在红外波段有差异的峰值区, 我们的测量值通常是介于Palmer和Williams的数据与Kou、Labrie和Chylek的数据之间, 且与后者接近。其中以1930 nm左右的水吸收系数波峰最为典型。由图3可以看出, 在1930 nm左右的水吸收系数波峰处, 本文的结果明显大于Palmer和Williams的结果, 而比Kou、Labrie和Chylek的略小, 三者在1925 nm处的值分别为: 13285、12400和13470。这是因为在测量一个特定波长范围水的吸收系数时, 很多学者容易倾向于增加被测水层的厚度, 以保证整体波长范围内的结果有较好的精度, 这会导致在高吸收峰波段透过水层的光能量的太小而超出了探测仪器的最佳探测范围, 从而造成吸收系数的测量数据不稳定。在我们的测量中, 所有光谱范围的吸收系数都确保在最佳的探测条件下测得, 所以测量结果更为稳定。

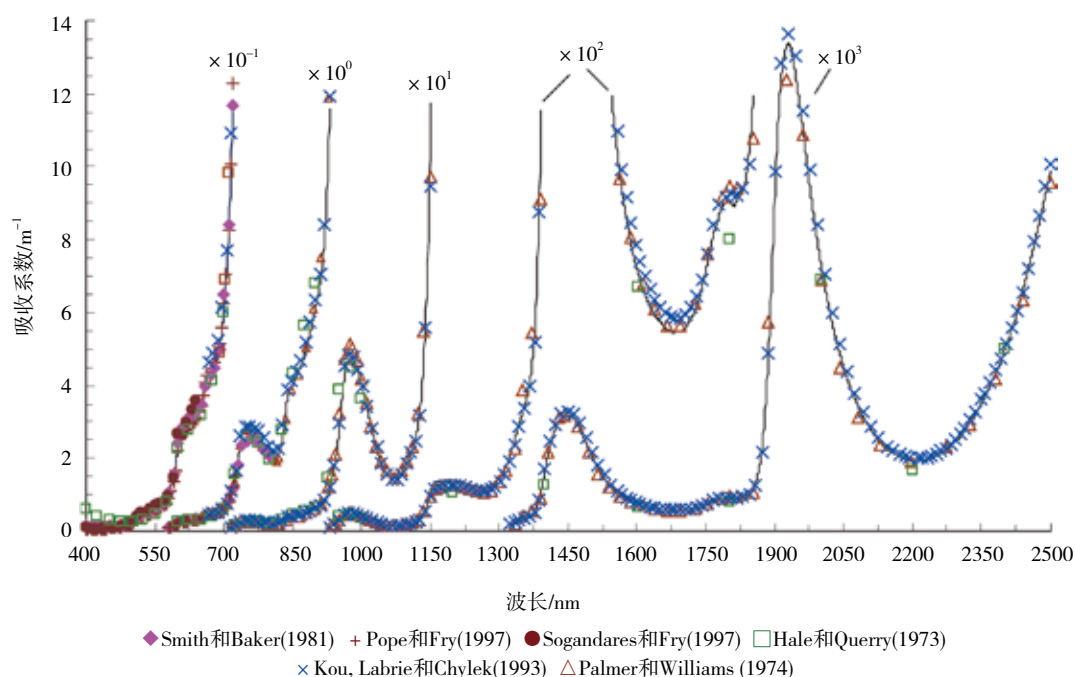


图3 本文所得的纯水400—2500 nm吸收系数(平滑曲线)与前人研究比较

4 总结

本文提出了一种测量红外波段纯水吸收系数光谱的新方法。该方法简单直接, 能够很好地控制被测量水层的厚度, 测量水层的厚度可在0.04—150 mm的区间变化, 因而所有的可见光波段和大部分红外波段都

能有效地测量。

利用比值法计算出水的吸收系数, 能有效地消除光源和探测设备等主要因素对结果的影响。

通过对厚度从0.04—150 mm的多个厚度水层进行测量, 并通过对各个水深最佳探测波段范围内测量数据的整合, 获得波长从900—2500 nm的纯水吸收系

数光谱，其结果精度可靠，且与被普遍接受的早期研究结果相一致。加上作者的前一篇文章《分离悬浮质影响的光学波段(400—900 nm)水吸收系数测量》的结果，给出了400—2500 nm的反射波段的纯水吸收系数，可作为相关定量遥感的基础数据。

参考文献(References)

Curcio J A and Petty C C. 1951. The near infrared absorption spectrum of liquid water. *Journal of the Optical Society of America*, 41(5): 302-304

邓孺孺, 何颖清, 秦雁, 陈启东, 陈蕾. 2012. 分离悬浮质影响的光学波段(400—900 nm)水吸收系数测量. *遥感学报*, 16(1): 174-191

Gordon H R. 1993. Sensitivity of radiative transfer to small-angle scattering in the ocean: quantitative assessment. *Applied Optics*, 32(36): 7505-7511

Hale G M and Querry M R. 1973. Optical constants of water in the 200nm to 200um wavelength region. *Applied Optics*, 12(3): 555-563

Kou L H, Labrie D and Chylek P. 1993. Refractive indices of water

and ice in the 0.65- to 2.5- μ m spectral range. *Applied Optics*, 32(19): 3531-3540

Marley N A, Gaffiney J S and Cunningham M M. 1994. Lambert absorption coefficients of water in the frequency range of 3000-934 cm-1. *Applied Optics*, 33(34): 8041-8054

Palmer K F and Williams D. 1974. Optical properties of water in the near infrared. *Journal of the Optical Society America*, 64(8): 1107-1110

Pope R M and Fry E S. 1997. Absorption spectrum (380—700 nm) of pure water. II. Integrating cavity measurements. *Applied Optics*, 36(33): 8710-8723

Smith R C and Baker K S. 1981. Optical properties of the clearest natural waters. *Applied Optics*, 20(2): 177-184

Sogandares F M and Fry E S. 1997. Absorption spectrum (340—640 nm) of pure water. 1. Photothermal measurements. *Applied Optics*, 36(33): 8699-8709

Tyler I L, Taylor G and Querry M R. 1978. Thin-wedge-shaped cell for highly absorbent liquids. *Applied Optics*, 17(6): 960-963

Wieliczka D M, Weng S S and Querry M R. 1989. Wedge shaped cell for highly absorbent liquids: infrared optical constants of water. *Applied Optics*, 28(9): 1714-1719

附录

吸收系数 α_w 和标准差 σ 表 (在纯水中它们是波长 λ 的函数)

λ/nm	α_w/m^{-1}	σ/m^{-1}	λ/nm	α_w/m^{-1}	σ/m^{-1}	λ/nm	α_w/m^{-1}	σ/m^{-1}
900	6.1884	0.0256	990	44.5386	1.1441	1080	14.9843	0.5006
905	6.5073	0.0235	995	42.4961	0.9612	1085	15.7179	0.5281
910	6.9042	0.0184	1000	40.0382	0.5827	1090	16.6783	0.5654
915	7.4607	0.0128	1005	37.4344	0.5687	1095	17.8467	0.5888
920	8.3139	0.0167	1010	34.7226	0.5942	1100	19.2845	0.5352
925	9.6392	0.0322	1015	31.7971	0.4985	1105	20.8313	0.5112
930	11.5774	0.0556	1020	28.9374	0.5549	1110	22.5262	0.5184
935	14.1677	0.0876	1025	26.2427	0.5029	1115	24.4669	0.5060
940	17.3963	0.1492	1030	23.8181	0.5161	1120	27.0585	0.5441
945	21.4374	0.2885	1035	21.6558	0.5049	1125	31.0228	0.6470
950	27.0426	0.2617	1040	19.6868	0.4859	1130	37.3991	0.8985
955	33.9925	0.5221	1045	18.0350	0.4833	1135	47.1984	1.3243
960	40.4604	0.8134	1050	16.7533	0.4719	1140	60.7775	2.0327
965	44.6345	1.0380	1055	15.7747	0.4739	1145	79.6172	1.6023
970	46.5729	1.2266	1060	15.0632	0.4630	1150	107.4252	3.6212
975	47.2258	1.4434	1065	14.6171	0.4657	1155	125.5627	3.8223
980	47.1185	1.1067	1070	14.4471	0.4698	1160	131.6432	3.9251
985	46.1659	1.2028	1075	14.5493	0.4951	1165	134.8601	3.9844

续表

λ/nm	α_w/m^{-1}	σ/m^{-1}	λ/nm	α_w/m^{-1}	σ/m^{-1}	λ/nm	α_w/m^{-1}	σ/m^{-1}
1170	136.6320	4.0448	1355	343.8465	6.9696	1540	1253.0276	15.7670
1175	137.6525	4.0541	1360	367.4948	7.2164	1545	1178.4295	15.2867
1180	138.5555	4.0835	1365	399.2005	7.5428	1550	1113.1924	14.8645
1185	139.4848	4.0822	1370	443.8689	7.9816	1555	1056.4427	14.4633
1190	140.4580	4.1114	1375	508.1205	8.5702	1560	1001.8636	14.0780
1195	140.7465	4.1106	1380	614.3273	10.8652	1565	947.6307	13.6833
1200	140.2052	4.1212	1385	791.0386	12.4317	1570	903.3081	13.3519
1205	139.2073	4.1050	1390	1037.7462	14.2865	1575	869.4973	13.1107
1210	137.7093	4.0651	1395	1338.3514	16.2805	1580	830.8426	12.7912
1215	136.1539	4.0459	1400	1671.4614	18.2428	1585	795.2601	12.5247
1220	134.5039	4.0094	1405	2004.7756	20.0347	1590	765.3087	12.2887
1225	132.5723	3.9777	1410	2299.4013	21.4677	1595	739.2764	12.0821
1230	130.8398	3.9402	1415	2546.4080	22.5945	1600	718.1947	11.8895
1235	129.0345	3.9052	1420	2742.4414	23.4508	1605	698.1034	11.7092
1240	127.1222	3.8697	1425	2888.7492	24.0617	1610	676.3345	11.5382
1245	125.4440	3.8483	1430	2998.7826	24.5045	1615	656.8966	11.3502
1250	123.9184	3.8271	1435	3077.4039	24.8265	1620	640.3602	11.2004
1255	122.6804	3.7974	1440	3125.9429	25.0176	1625	624.4244	11.0867
1260	121.8107	3.7821	1445	3149.9303	25.1116	1630	612.9789	10.9950
1265	121.6186	3.7675	1450	3159.1215	25.1574	1635	600.3195	10.8386
1270	121.9652	3.7863	1455	3145.7882	25.0872	1640	587.2072	10.7111
1275	123.1212	3.8046	1460	3104.6653	24.9376	1645	581.5459	10.6964
1280	125.4438	3.8587	1465	3032.2772	24.6450	1650	576.4747	10.6264
1285	128.5339	3.9124	1470	2921.7997	24.1834	1655	566.8229	10.5321
1290	132.9452	4.0090	1475	2789.9066	23.6105	1660	557.8632	10.4569
1295	138.8124	4.1269	1480	2649.0557	23.0134	1665	552.4071	10.4134
1300	145.8619	4.2425	1485	2503.1788	22.3575	1670	550.8155	10.4267
1305	154.6123	4.4000	1490	2359.6925	21.7063	1675	546.4029	10.2933
1310	165.8897	4.5936	1495	2216.7008	21.0201	1680	545.7660	10.3457
1315	179.8041	4.8251	1500	2083.1254	20.3850	1685	548.7931	10.3422
1320	195.9858	5.0714	1505	1955.5434	19.7313	1690	550.1508	10.3955
1325	214.5301	5.3591	1510	1828.2567	19.0580	1695	548.1242	10.3343
1330	235.1264	5.6463	1515	1707.3415	18.4441	1700	551.5667	10.4226
1335	257.4468	5.9333	1520	1598.2384	17.8236	1705	557.4718	10.4550
1340	280.2109	6.2337	1525	1501.0728	17.2870	1710	567.9853	10.5116
1345	301.8872	6.4778	1530	1411.4466	16.7300	1715	580.7795	10.6598
1350	322.9455	6.7370	1535	1330.0455	16.2448	1720	588.9609	10.7467

续表

λ/nm	α_w/m^{-1}	σ/m^{-1}	λ/nm	α_w/m^{-1}	σ/m^{-1}	λ/nm	α_w/m^{-1}	σ/m^{-1}
1725	600.8988	10.8644	1910	11785.0118	48.7745	2095	3080.8073	24.7402
1730	619.2023	11.0118	1915	12538.9739	50.2398	2100	2979.6127	24.3419
1735	640.1112	11.1797	1920	13019.8819	51.1522	2105	2881.9971	23.9525
1740	666.0047	11.4651	1925	13284.4851	51.7008	2110	2775.0513	23.4428
1745	689.4827	11.6367	1930	13377.2446	51.8120	2115	2692.1798	23.1439
1750	717.1088	11.8595	1935	13284.6730	51.6623	2120	2611.2278	22.7564
1755	752.7150	12.1704	1940	12985.2155	51.0066	2125	2526.6678	22.4146
1760	780.9415	12.3969	1945	12569.8817	50.2162	2130	2439.7979	21.9963
1765	809.3959	12.6638	1950	12121.3278	49.2982	2135	2367.2879	21.6851
1770	831.2326	12.8079	1955	11660.7820	48.3564	2140	2312.0539	21.4561
1775	849.2241	12.9889	1960	11174.4059	47.3403	2145	2256.0577	21.1354
1780	873.9375	13.1127	1965	10658.6376	46.1908	2150	2215.8617	20.9544
1785	894.0727	13.3086	1970	10110.3070	44.9694	2155	2177.0876	20.8096
1790	898.4171	13.3062	1975	9587.2335	43.8239	2160	2130.1240	20.5180
1795	902.1133	13.3612	1980	9093.3448	42.6545	2165	2099.8806	20.4763
1800	905.1582	13.3709	1985	8638.8885	41.5737	2170	2053.4546	20.1573
1805	899.7925	13.3183	1990	8201.0527	40.4800	2175	2024.7078	20.0260
1810	891.7933	13.2702	1995	7770.3487	39.4536	2180	2015.4595	20.0432
1815	901.2435	13.2675	2000	7364.6545	38.3348	2185	1995.7610	19.8553
1820	916.9734	13.4471	2005	6994.7081	37.3859	2190	1967.3868	19.7351
1825	922.1306	13.4119	2010	6647.0382	36.4063	2195	1944.7839	19.6313
1830	934.6580	13.4713	2015	6327.5106	35.5869	2200	1947.3039	19.6494
1835	953.4940	13.6030	2020	6007.5693	34.6112	2205	1953.0090	19.6160
1840	994.0810	13.9207	2025	5700.9784	33.7455	2210	1976.9291	19.8194
1845	1056.5967	14.3174	2030	5421.2357	32.8879	2215	1967.1752	19.6807
1850	1132.9730	14.8648	2035	5183.3520	32.1964	2220	1962.5190	19.7697
1855	1243.1728	15.5692	2040	4953.4561	31.4398	2225	1962.7188	19.6689
1860	1415.7472	16.6691	2045	4726.1692	30.7026	2230	1958.9635	19.7425
1865	1664.4644	18.0279	2050	4512.3844	30.0040	2235	1992.9890	19.8530
1870	2067.3102	20.1143	2055	4302.5010	29.3131	2240	2032.2671	20.0908
1875	2678.7960	22.9734	2060	4114.0033	28.6546	2245	2038.9316	20.1235
1880	3500.1258	26.3717	2065	3949.8433	28.0594	2250	2070.8117	20.2535
1885	4593.0215	30.1578	2070	3791.7650	27.4838	2255	2110.6788	20.4194
1890	5992.0760	34.5577	2075	3636.0017	26.9347	2260	2137.1224	20.5265
1895	7566.6078	38.9982	2080	3483.4019	26.3476	2265	2172.9845	20.7662
1900	9196.2681	43.0143	2085	3335.0891	25.7767	2270	2207.9950	21.0225
1905	10673.2160	46.3941	2090	3199.6813	25.2807	2275	2248.7080	21.0766

续表

λ/nm	α_w/m^{-1}	σ/m^{-1}	λ/nm	α_w/m^{-1}	σ/m^{-1}	λ/nm	α_w/m^{-1}	σ/m^{-1}
2280	2299.6275	21.3013	2355	3642.7963	27.1051	2430	6106.4604	34.9973
2285	2373.7696	21.7304	2360	3770.5952	27.3852	2435	6342.7058	35.1967
2290	2442.6123	22.0061	2365	3890.6802	27.8528	2440	6583.8864	35.8459
2295	2491.4185	22.2091	2370	4015.3320	28.3421	2445	6830.0022	36.8070
2300	2548.7591	22.6158	2375	4165.6284	28.7980	2450	7081.0532	37.3600
2305	2600.9227	22.7054	2380	4282.6965	29.2605	2455	7337.0394	38.0974
2310	2694.8454	23.1953	2385	4426.6887	29.6833	2460	7597.9608	38.9928
2315	2789.5631	23.5403	2390	4603.4652	30.2149	2465	7863.8175	39.2615
2320	2887.5870	23.9247	2395	4794.8223	30.9753	2470	8134.6093	40.3983
2325	3009.1713	24.3983	2400	5032.0681	31.6918	2475	8410.3364	42.0815
2330	3077.0556	24.8207	2405	5170.8675	32.1701	2480	8690.9987	40.1862
2335	3151.8896	25.0671	2410	5266.7612	32.2945	2485	8976.5962	43.7344
2340	3289.8315	25.6099	2415	5519.1696	33.2164	2490	9267.1289	39.5020
2345	3408.2837	26.0753	2420	5695.1827	33.6903	2495	9562.5969	42.0205
2350	3522.2109	26.3853	2425	5886.0474	34.2915	2500	9863.0000	43.8201